World Academy of Science, Engineering and Technology
International Journal of Physical and Mathematical Sciences
Vol:12, No:9, 2018

Specific Frequency of Globular Clusters in Different Galaxy Types

Ahmed H. Abdullah, Pavel Kroupa

***Abstract*—**Globular clusters (GC) are important objects for tracing the early evolution of a galaxy. We study the correlation between the cluster population and the global properties of the host galaxy. We found that the correlation between cluster population (N_{GC}) and the baryonic mass (M_b) of the host galaxy are best described as $10^{-5.6038}M_b$. In order to understand the origin of the U -shape relation between the GC specific frequency (S_N) and M_b (caused by the high value of S_N for dwarfs galaxies and giant ellipticals and a minimum S_N for intermediate mass galaxies$\approx 10^{10}M\odot$), we derive a theoretical model for the specific frequency (S_{Nth}). The theoretical model for S_{Nth} is based on the slope of the power-law embedded cluster mass function (β) and different time scale (Δt) of the forming galaxy. Our results show a good agreement between the observation and the model at a certain β and Δt. The model seems able to reproduce higher value of S_{Nth} of $\beta = 1.5$ at the midst formation time scale.

***Keywords*—**Galaxies, dwarf, globular cluster, specific frequency, formation time scale.

I. Introduction

GLOBULAR clusters (GCs) are spherical concentrations of stars (10^4_10^7 stars), which are made up of population II objects (i.e., old stars) and are regarded as one of first stellar systems to form in the early Universe. The luminosity and compact size (half-light radii of a few pc) of GCs lead to the brightest objects that can be recognized around galaxies out to galactocentric radii $\approx$ 200 kpc [1]. Globular clusters are found within different morphological types of galaxies, from irregulars to spiral and elliptical galaxies. Probably most of the GCs formed at the same time as their host galaxy, so that the global properties of the GCs can be considered as a key object to study the formation and evolution of galaxies. For the purpose of developing an understanding of the formation efficiency of globular clusters as a function of galaxy luminosity (or mass), their total number normalized to specific frequency S_N. Specific frequency which is the number of globular clusters N_{GC} per unit V-band luminosity, normalized at $Mv = -15$ [2]

$$S_N = N_{GC}10^{0.4(M_v+15)} \tag{1}$$

This simple parameter S_N was introduced by Harris and van den Bergh [2] as a measure of the richness of a GC system normalized to the host galaxy luminosity. This measure shows that the S_N varies between galaxies of different morphological type. The spiral galaxies have S_N between 0.5 to 2 [3]-[5]. For more luminous ellipticals galaxies the S_N ranges from $\approx$ 2 to 10 and tends to increase with luminosity. The S_N increases from few to several dozen for early-type dwarfs galaxies [6]-[8], and for late type dwarfs galaxies [9], [10].

The S_N is affected by environments, for dEs galaxy in denser environments S_N is higher while for Es galaxy in rich cluster is smaller [11]-[14]. The cD galaxy (central dominant elliptical galaxy) having S_N value larger than 10 [15], [16]. Forbes et al. [17] proposed a tidal stripping model of GCs from smaller galaxies to explain the increasing value of S_N in cD galaxies. In this work, we construct a model to calculate the theoretical specific frequency (S_{Nth}) for early type galaxies depending on the slope of the embedded cluster mass function (β) and different formation time scale of the galaxy (Δt). The effect of these two parameters β and Δt on S_{Nth} will be investigated. The outline of this paper is as follows: the description of theoretical specific frequency S_{Nth} is presented in Section II. Comparison between the observed data and S_{Nth} is presented in Section III. Finally Section IV contains our discussion and conclusion.

II. Theoretical Specific Frequency (S_{Nth})

According to (1) we derive an analytical model for the theoretical specific frequency S_{Nth}, which is the number of globular clusters N_{GC} per unit luminosity or (Mv), the galaxy magnitude (Mv) can by converted into a mass (M_{gal}) by using mass-to-light-ratio ψ,

$$S_{Nth} = \frac{N_{GC}}{M_{gal}} \times \psi 10^6 \tag{2}$$

Beginning with a power-law globular cluster mass function (CMF),

$$\xi_{ecl}(Mecl) = K_{ecl}M_{ecl}^{-\beta} \tag{3}$$

where ξ_{ecl} is the mass function of embedded cluster and K_{ecl} is the normalization constant, here we constrain the power law slope of the (CMF) β between (1.5 _ 2.5) [18]-[20]. Using the empirical relation which derived by [20], which represents the relation between the maximum cluster mass $(M_{ecl,max})$ and the star-formation rate (SFR) of the host galaxy based on a linear regression fit to the observational data from [21] for absolute magnitude (Mv) of the brightest young cluster and star formation rate.

$$M_{ecl,max} = K_{ML}SFR^{0.75} \times 10^{6.77} \tag{4}$$

Ahmed H. Abdullah is with the Department of Astronomy, College of Science, University of Baghdad, Baghdad, 10071, Iraq (e-mail: vipahmed.hasan@gmail.com).

Pavel Kroupa is with the Argelander Institut für Astronomie der Universität Bonn, Auf dem Hügel 71, D-53121 Bonn, Germany, Helmholtz-Institut fuer Strahlen- und Kernphysik, Universität Bonn, Nussallee 14-16, D-53115 Bonn, Germany.

where $K_{ML} = 0.0144$ is the typical mass-to-light-ratio for young globular cluster population [20], [22]. The total mass of a population of star cluster M_{gal} is,

$$M_{gal} = \int_{M_{ecl,min}}^{M_{ecl,max}} \xi_{ecl}(Mecl) M_{ecl} dM_{ecl} \tag{5}$$

where $M_{ecl,min}$ is the minimal mass of a star cluster which can be expressed as 5M$\odot$ which is the lower mass observed in the Taurus-Auriga aggregate [23], [20].

Using (3) and (5) at $\beta \neq 2$, in order to determine the normalization constant K_{ecl}

$$K_{ecl} = \frac{M_{gal} \times (2-\beta)}{(M_{ecl,max})^{(2-\beta)} - (5M\odot)^{(2-\beta)}} \tag{6}$$

The number of GC (N_{GC}), can also be expressed with the CMF at a minimum cluster mass which we take to be $10^4 M\odot$, as Baumgardt and Makino [24] suggested this as the minimum mass remaining bound as a cluster after 13 Gyr.

$$N_{GC} = \int_{10^4 M\odot}^{M_{ecl,max}} \xi_{ecl}(Mecl) M_{ecl} dM_{ecl} \tag{7}$$

putting (3) into (7) then,

$$N_{GC} = \frac{K_{ecl}}{1-\beta}[M_{ecl,max}^{(1-\beta)} - (10^4 M\odot)^{(1-\beta)}] \tag{8}$$

Substituting the value for K_{ecl} from (6), we have

$$N_{GC} = M_{gal} \frac{2-\beta}{1-\beta} \frac{M_{ecl,max}^{(1-\beta)} - (10^4 M\odot)^{(1-\beta)}}{M_{ecl,max}^{(2-\beta)} - (5M\odot)^{(2-\beta)}} \tag{9}$$

From (4) we substitute the $M_{ecl,max}$, when SFR is depends on time and on mass. Having obtained N_{GC} and M_{gal} the S_{Nth} follows from

$$S_{Nth} = \frac{2-\beta}{1-\beta} \times \frac{[(SFR)^{0.75} \times K_{ML} \times 10^{6.77}]^{(1-\beta)} - (10^4 M\odot)^{(1-\beta)}}{[(SFR)^{0.75} \times K_{ML} \times 10^{6.77}]^{(2-\beta)} - (5M\odot)^{(2-\beta)}} \times \psi 10^6 M\odot \tag{10}$$

where $SFR = M_b/\Delta t$ here (M_b) is the baryonic mass and Δt is the formation time scale.

The E and dE galaxies formed under different physical boundary conditions [25], [26], which need different formation time-scales. In Fig. 1 we show the theoretical specific frequency from equation (10) as a function of baryonic mass (M_b) with CMF power law indices $\beta = 2.3$. We have tested eight values of Δt_S ranging from 10^3 to 10^{10} yr, also assume $\psi = 1$ (mass -to-light ratio for the galaxy), we will see later whether this assumption was reasonable. In these calculations we ignore any value of S_{Nth} that are zero or negative. Here $\beta = 2.3$ which agrees with the work of [20] and later we continuum of slop in the range between $(1.5-2.5)$ to include the entire slopes. It is clearly indicates the trend of S_{Nth}, at lower mass the higher scale time deviations are stronger, which is also notice S_{Nth}, remained constant =2.4 for high

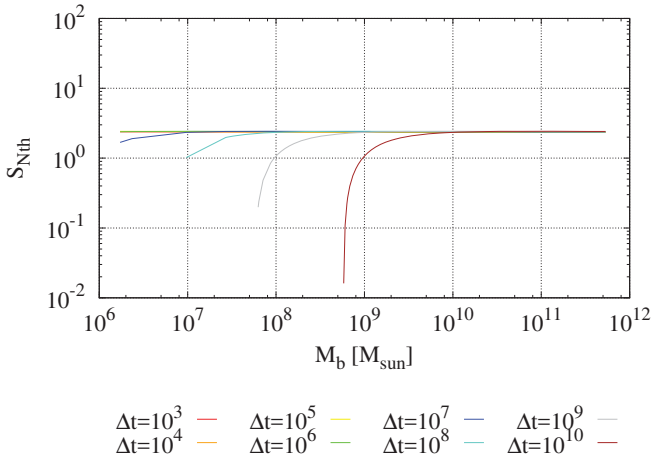

Fig. 1 Theoretical specific frequency S_{Nth} versus wide range of galaxy mass M_b. Color selected from left to right represent increasingly different formation time scale of the galaxy (Δt) ranging from flatter to curves ($10^3, 10^4, 10^5, 10^6, 10^7, 10^8, 10^9$and 10^{10}) yr, assume $\psi = 1$ (mass-to-light ratio for the galaxy) and CMF with $\beta = 2.3$

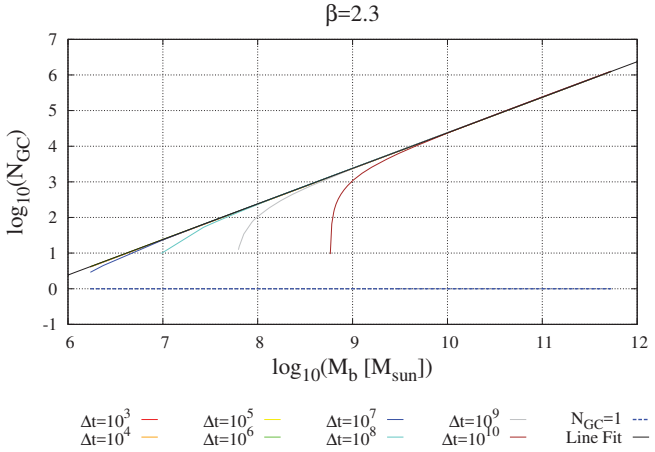

Fig. 2 The number of GCs versus the baryonic mass of galaxy for different time of galaxy formation (10^3 to 10^{10}) yr (uppermost to lowermost curves), at β = 2.3 and ψ =1. The blue line corresponds to the one GC (N_{GC}=1). The black line is the best-fit line (11)

mass of galaxy $M_b > 10^{10} M\odot$, on this basis and according to equation (2) the N_{GC} is approximately proportional to M_{gal}.

The correlation between the N_{GC} and M_b which is demonstrated in Fig. 2 shows as expected previously a linear (log scale) in behavior at high mass of galaxy $M_b > 10^{10} M\odot$ which is achieved independent of Δt and also shifted by one power of ten for small M_b. We derive a best-fit relation (black line):

$$log_{10}(N_{GC}) = log_{10}(M_b) + b \tag{11}$$

where $b = -5.6038$ the $log_{10}(N_{GC})$ - intercept

$$N_{GC} = 10^{-5.6038} M_b \tag{12}$$

Equation (2) can be expressed with (12) as

$$S_{Nth} = \frac{10^{-5.6038} M_b}{M_b} 10^6 \tag{13}$$

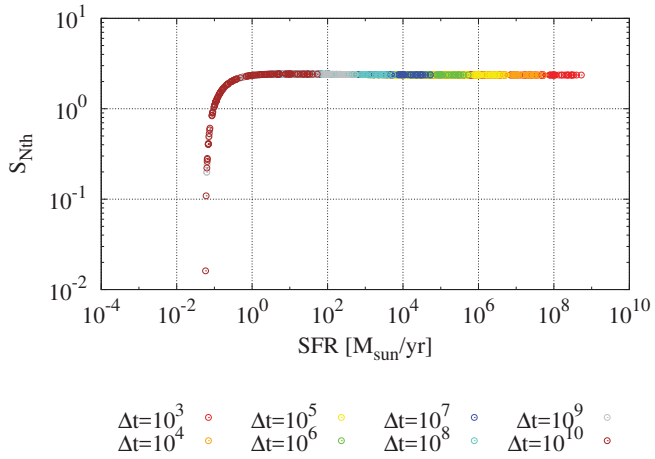

Fig. 3 Theoretical Specific frequency, S_{Nth}, versus the star formation rate (SFR) of host galaxy, the different colors of circles mark galaxies with different formation time (Δt) range from 10^3 to 10^{10} yr, $SFR = M_b/\Delta t$ remained constant for $SFR > 1M\odot/yr$

S_{Nth} = 2.48 is similar to the previous value in Fig. 1 when S_{Nth}, remained constant =2.4 for high mass of galaxy.

If we compare between equations 9 and 12, we find the origin of the proportionality, we can see that the fraction term must be constant. The term with $M_{ecl,max}$ (SFR) in the numerator of the formula will be reduced by about an order of magnitude when M_{gal} is increased by a factor of ten.The situation is similar for the denominator, but the term M_{max} (SFR) does not fall so strongly with Mgal and here always smaller than $(5M\odot)^{2-\beta}$

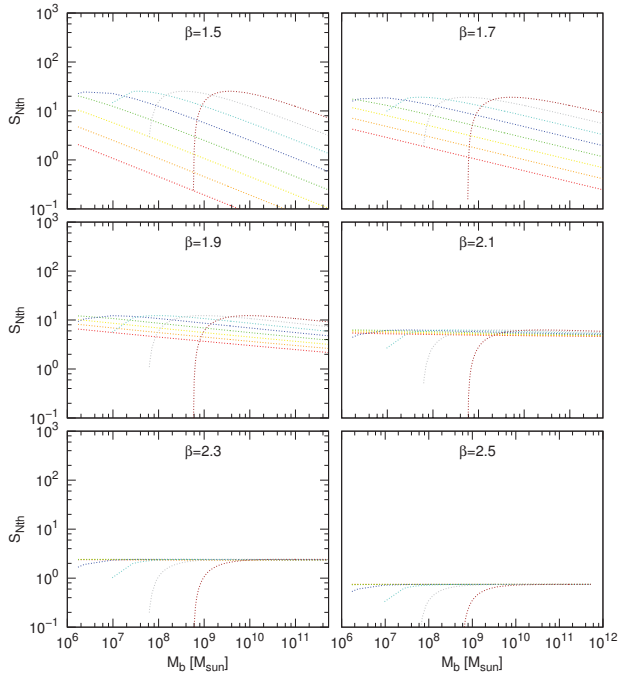

Fig. 4 Theoretical specific frequency S_{Nth} versus wide range of galaxy mass M_b for different value of β. The coloured dot lines indicate different formation time scale (as in Fig. 1)

Fig. 3 shows how long it take this galaxy to form at a given mass, it also can be seen that the specific frequency S_{Nth} behaves largely independently of the SFR i.e. The different formation time does not influence any of the results.

We compared the formation time Δt_{MW} for the Milky Way (MW) which has a known specific frequency with the literature values Δt_{MW} = (0.5 - 1) Gyr [27]. At a given specific frequency S_{Nth} for MW (2.3) and with mass M_{MW} = $10^8 M\odot$, which is estimated from the mass of the old population II spheroid, which together with the GC, at a certain value of β= 2.3, mass-to-light-ratio = 1 and N_{GC} =150. Having obtained this values, and after calculating equation 10 numerically, the Δt_{MW} equal 7.058e+08 yr (0.705 Gyr). This value lies exactly in the range Δt_{MW} = 0.5 - 1 Gyr [27], and shows that the model with ψ = 1 gives the correct physical leading results. In this work we assume 6 values of the power low slope of the (CMF) β: 1.5, 1.7, 1.9, 2.1, 2.3 and 2.5. To better estimate the difference between various models, we have plotted in Fig. 4 the S_{Nth} versus baryonic mass for a singular case to the power law slope of the (CMF) in the range β between (1.5 - 2.5), for each plot we assume eight possible values of different formation time ranging from 10^3 to 10^{10} (red to brown). It can be clearly seen that the lines become separate from each other at a low mass, while for high mass $>$ (10^{10}) they become flatter at β (2.1, 2.3 and 2.5) and disperse at β (1.5, 1.7 and 1.9). Thus we see how the results are sensitively dependent on the power law index β. Fig. 5 shows the same behavior of β for a range between (1.5 - 2.5) and different formation times which ranging from 10^3 to 10^{10} same as Fig. 4 but for N_{GC} and mass of galaxies.

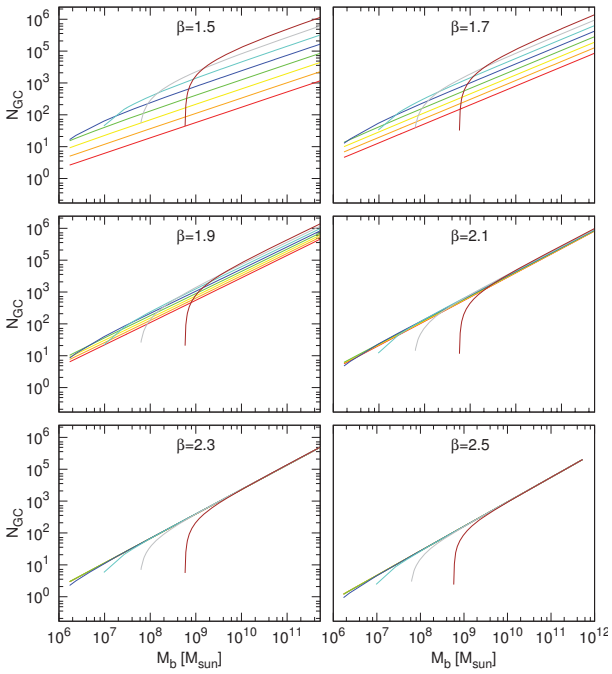

Fig. 5 Number of globular cluster N_{GC} versus mass of galaxy for different formation time scale (as in Fig. 2) and for different value of β

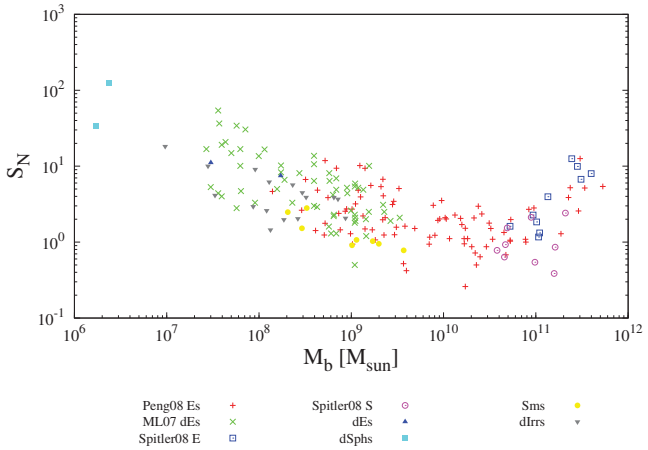

Fig. 6 The specific frequency of globular cluster versus baryonic mass for a range of galaxy morphologies. The various symbol type and colours which explained in the figure legend, represent different sources of data: red plus signs (ellipticals) from [7], green crosses (dwarf ellipticals) from [6], blue squares (elliptical) [32], pink circles (spiral) [32]. While for nearby dwarf galaxies blue solid triangles (dEs), cyan solid square (dSphs), yellow solid circles(Sms) and grey solid triangles (dIrrs) from [33], [34]

III. Comparison between the Observed Data and Theoretical Specific Frequency(S_{Nth})

The specific frequencies of GCs (S_N) are important tools for the aim of understanding the evolution of the galaxies [28], [13]. In Fig. 6 we show the observed samples of galaxies (the main source of this data is [8]), we demonstrate the general tendency of the specific frequency of GCs (S_N) versus range of galaxy mass ($M_V = -11$ to-23 mag), which takes a 'U' -shape as usual. At the low -mass and high- mass end of the scale, the S_N value is higher compared with the galaxy at intermediate mass which becames close to one. The value of S_N is high in dwarf spheroidal (dSph) galaxies in contrast to spiral galaxies which have smaller S_N. We also notice that the S_N of giant elliptical is higher than for giant spirals, which is due to the formation of globular cluster during collision of spiral galaxies which forms ellipticals [29]-[31]. S_N for dSphs (low mass) is higher than dwarf irregular (dIrs), which might suggest that dSphs progenitors of dIrss and dEs [35], [8]. The general trend is towards increasing S_N above and below Mv$\approx$ -20 mag ($\approx$ 4.7 $\times 10^{10} M\odot$), regardless the galaxy type [8]. The median for the whole sample is (S_N=2.56) and 58% of the sample are located below S_N=3.

IV. Discussion and Conclusions

We investigated the correlation between(S_N) and baryonic mass, which shows a 'U'-shape, the (S_N) value is higher for dwarfs and supergiants (the low and high- mass end of the scale) compared to the galaxy at intermediate mass which take value nearly to one. The population (N_{GC}) correlates linear (log scale) with (N_{GC}) at high mass of galaxy $M_b > 10^{10} M\odot$. This agrees with previous studies that suggest that the specific frequency (S_N) is a function of galaxy mass, which holed irrespective of galaxy morphology.

The Comparison between the data in Fig. 6 and the theoretical specific frequency, we performed the model at 6

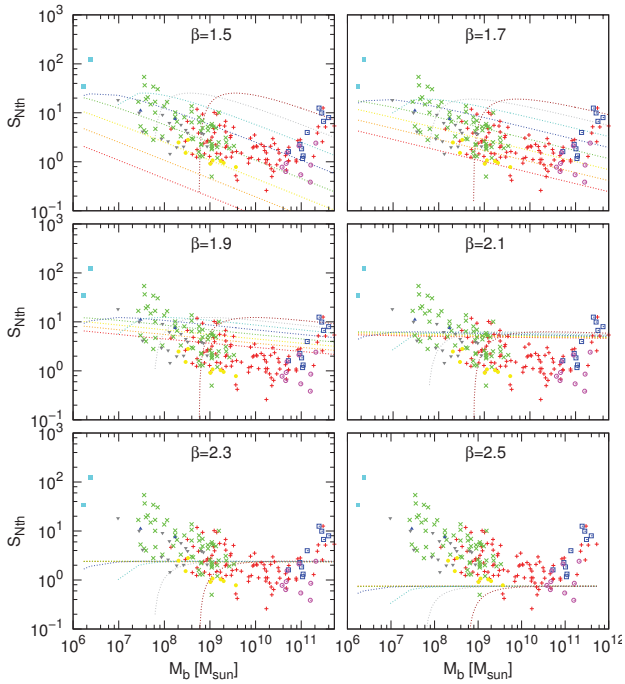

Fig. 7 Comparison between the observed Data and model with different β and different formation time

different a simple power law index β ranging from (1.5 to 2.5) and for eight different formation time scale (Δt), that can be understood as being due to the observation of entire galaxy population instead of individual galaxies. In addition the mass of galaxy varies with the formation time scale. The low mass with high S_N is identical to short formation time scale which can be described with small β while high mass with low (S_N) is better described by high β. In Fig. 7 we show our results for S_{Nht} as a function of the M_b for different values of β and different formation time scale and compare our models with observational data.

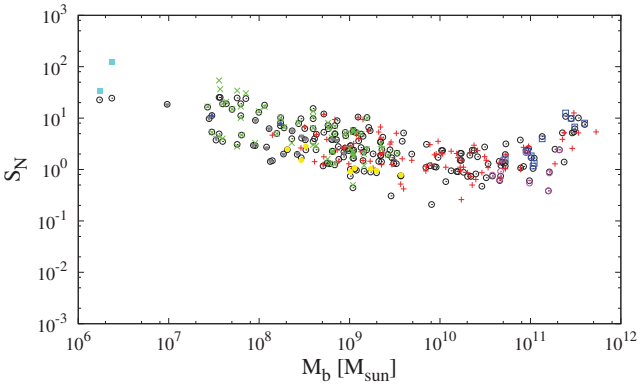

Fig. 8 Specific frequency (S_N) versus baryonic mass (M_b). Black circles represents the model with best value of different formation time and β which explain the observation data. The various symbol types as in the Fig. 6

The model with β = 2.1, 2.3 and 2.5 can reproduce the data for the specific frequency smaller than 6.2, 2.4, 0.74

respectively and the models with β = 1.5 , 1.7 and 1.9 agree with the S_{Nth} for a wide range of Δt. The model with β =2.5 fail to fit the most data galaxy especially at $S_N > 0.74$, and also all model for Δ t = 10^{10} are biased towards high mass, therefore fail also to fit the data at low mass.

Furthermore, all the models except β= 2.5 predict the specific frequency significantly for Sms and S galaxies while the models at 1.5, 1.7 and 1.9 predict the S_N for the vast majority of S_N for the Es, ML07 dEs, E, dEs, dIrrs, galaxies.

However, we point out that the model with β= 1.5 produces a larger range of S_{Nth} which fits the data much better, and for the models β =1.5 and β =1.7 the mildest Δt can reproduce the high S_{Nht}, We also see a possible hint that the embedded cluster mass function may become top-heavy (smaller β) in major galaxy-wide star burst, which was also suggested by [36]. In Fig. 8 shows the observational data and a best value of β and Δt which is obtained by measuring the smallest vertical distance between the data and model $distance = \mid S_N - S_{Nth} \mid$. The histogram distributions in Fig. 9 shows the number of best value of β at a period time which can explain the specific frequency of observed data and illustrates that the β= 1.5 best value to explains the observed data . The maximum theoretical specific frequency characterized by a specific β at a given formation time scale is shown in Fig. 10. Nevertheless, some dwarfs stand out as having high S_N which also can be described by β smaller than that we use in our calculations. With smaller β we get correspondingly higher specific frequencies, and to get extension must include galaxies which are formed in a starburst, such as elliptical and dwarf elliptical galaxies.

The Milky Way appear to be in the formation time scale t_{MW} equal to 0.705 Gyr according to the S_{Nth} relation.

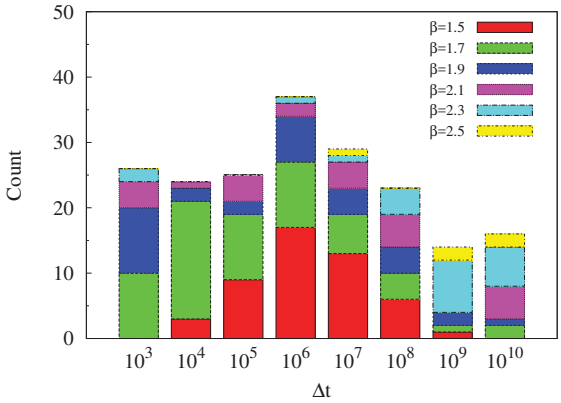

Fig. 9 The histogram for the best β at a different time scale which can explain the specific frequency of observed data. The coloured bars are explained in the figure legend

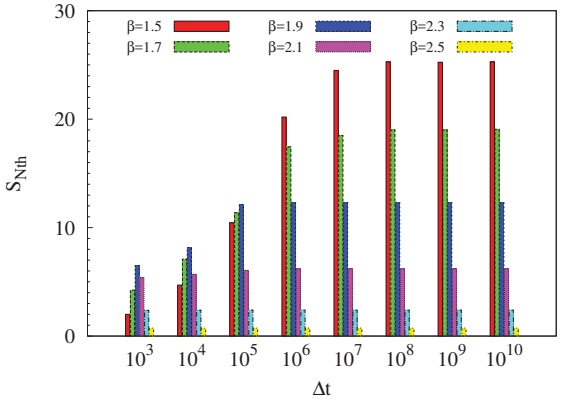

Fig. 10 The maximum theoretical specific frequency versus formation time scale at a different value of β. The coloured bars are explained in the figure legend

ACKNOWLEDGMENT

We would like to thank S. Unruh, M. Kruckow, A. Dieball and L. AL-Mashhadani for their useful discussions and suggestions and I. Georgiev for providing data. The research was supported by the Ministry of Higher Education and Scientific Research of Iraq (MoHESR), and by the Deutscher Akademischer Austauschdienst (DAAD).

REFERENCES

[1] Spitler, L. R., Romanowsky, A. J., Diemand, J., Strader, J., Forbes, D. A., Moore, B., & Brodie, J. P. 2012, , 423, 2177.
[2] Harris, W. E. & van den Bergh, S. 1981, , 86, 1627.
[3] Goudfrooij, P., Strader, J., Brenneman, L., Kissler-Patig, M., Minniti, D., & Edwin Huizinga, J. 2003, , 343, 665.
[4] Chandar, R., Whitmore, B., & Lee, M. G. 2004, , 611, 220.
[5] Rhode, K. L., Zepf, S. E., Kundu, A., & Larner, A. N. 2007, , 134, 1403.
[6] Miller, B. W. & Lotz, J. M. 2007, , 670, 1074.
[7] Peng, E. W., Jordán, A., Côté, P., Takamiya, M., West, M. J., Blakeslee, J. P., Chen, C.-W., Ferrarese, L., Mei, S., Tonry, J. L., & West, A. A. 2008, , 681, 197.
[8] Georgiev, I. Y., Puzia, T. H., Goudfrooij, P., & Hilker, M. 2010, , 406, 1967.
[9] Sharina, M. E., Puzia, T. H., & Makarov, D. I. 2005, , 442, 85.
[10] Georgiev, I. Y., Goudfrooij, P., Puzia, T. H., & Hilker, M. 2008, , 135, 1858.
[11] Hanes, D. A. 1977, , 84, 45.
[12] Durrell, P. R., Harris, W. E., Geisler, D., & Pudritz, R. E. 1996, , 112, 972.
[13] Brodie, J. P. & Strader, J. 2006, , 44, 193.
[14] Harris, W. E., Harris, G. L. H., & Alessi, M. 2013, , 772, 82.
[15] West, M. J., Cote, P., Jones, C., Forman, W., & Marzke, R. O. 1995, , 453, L77.
[16] Alamo-Martínez, K. A., Blakeslee, J. P., Jee, M. J., Côté, P., Ferrarese, L., González-López lira, R. A., Jordán, A., Meurer, G. R., Peng, E. W., & West, M. J. 2013, , 775, 20.
[17] Forbes, Brodie, & Grillmair 1997 .
[18] Elmegreen, B. G. & Efremov, Y. N. 1997, , 480, 235. Forbes, D. A., Brodie, J. P., & Grillmair, C. J. 1997, , 113, 1652
[19] Kroupa, P. & Weidner, C. 2003, , 598, 1076.
[20] Weidner, C., Kroupa, P., & Larsen, S. S. 2004, , 350, 1503.
[21] Larsen, S. S. 2002, , 124, 1393.
[22] Smith, L. J. & Gallagher, J. S. 2001, , 326, 1027.
[23] Briceño, C., Luhman, K. L., Hartmann, L., Stauffer, J. R., & Kirkpatrick, J. D. 2002, , 580, 317.
[24] Baumgardt, H. & Makino, J. 2003, , 340, 227
[25] Okazaki, T. & Taniguchi, Y. 2000, , 543, 149
[26] Dabringhausen, J. & Kroupa, P. 2013, , 429, 1858.
[27] Marks, M. & Kroupa, P. 2010, , 406, 2000.
[28] Harris, W. E. 1991, , 29, 543.
[29] Schweizer, F. 1987, in Nearly Normal Galaxies. From the Planck Time to the Present, ed. S. M. Faber, 18–25.
[30] Ashman, K. M. & Zepf, S. E. 1992, , 384, 50.
[31] Zepf, S. E. & Ashman, K. M. 1993, , 264, 611.
[32] Spitler, L. R., Forbes, D. A., Strader, J., Brodie, J. P., & Gallagher, J. S. 2008, , 385, 361.
[33] Georgiev, I. Y., Hilker, M., Puzia, T. H., Goudfrooij, P., & Baumgardt, H. 2009, , 396, 1075.
[34] Georgiev, I. Y., Puzia, T. H., Hilker, M., & Goudfrooij, P. 2009, , 392, 879.

[35] Miller, Lotz, Ferguson, Stiavelli, & Whitmore.
[36] Weidner, C., Kroupa, P., Pflamm-Altenburg, J., & Vazdekis, A. 2013, , 436, 3309.